Estimation of direct and indirect economic losses

caused by a flood with long-lasting inundation:

application to the 2011 Thailand flood

M. Tanoue[1]†, R. Taguchi[2], S. Nakata[2], S. Watanabe[2], S. Fujimori[3], Y. Hirabayashi[1]

[1]Department of Engineering, Shibaura Institute of Technology, Japan.

[2]Graduate School of Engineering, The University of Tokyo, Japan.

[3]Graduate School of Engineering, Kyoto University, Japan.

Corresponding author: Masahiro Tanoue (tanoue.masahiro.s6@sic.shibaura-it.ac.jp)

†3-7-5 Toyosu, Koto-ku, Tokyo, Japan, 135-8548.

Key Points

- A modeling framework to estimate the direct and indirect economic losses due to a

  flood with long inundation period were developed.

- We applied the modeling framework for the 2011 Thailand flood and showed long-

  term indirect economic losses.

- Our modeling framework help us to understand various types of flood risk on

  economy for both short- and long-term time scales.

Abstract

River floods are common natural disasters, causing serious economic damage

worldwide. In addition to direct assets damage such as destruction of physical assets,

floods with long-lasting inundation cause direct and indirect economic losses in and

outside the affected area. Direct economic losses include opportunity losses such as

business interruption and the cost of emergency measures such as cleaning, while

indirect economic losses emerge as effects to several sectors within the trade and supply

network. At this moment, there are limited studies to explicitly estimate the direct and

indirect economic losses at global scale due to limitation in modeling inundation depth

and period at finer scales. Here, we develop a global modeling framework to estimate

the direct and indirect economic losses using a computable general equilibrium model and a global river and inundation model, which is appropriately reproduced inundation depth and periods. Application of the method to the 2011 Thailand flood demonstrated that the estimated economic losses due to business interruption and recovery in the industry and service sectors totaled $19.5 billion, which was similar to the estimated direct assets damage of the flood ($22.0 billion). The estimated indirect economic losses reduced the GDP of the country by 5.48% in 2011, and will cause more than 0.5% reduction of the GDP even in 2030, resulting in $55.3 billion of total losses for 2011-2030. We reveals that comprehensive estimation of direct and indirect economic losses help to understand various types of flood risk on economy for both short- and long-term time scales.

1. Introduction

River floods are a major climate disaster, leading to serious economic consequences at a global scale. Between 1990 and 2013, the Emergency Events Database of the Center for Research on the Epidemiology of Disasters (EM-DAT) reported that the global total economic losses exceeded $526 billion at purchasing power parity (PPP) values (base year 2005). Flood risks are expected to increase steeply with socioeconomic developments and climate change (e.g., Arnell and Lloyd-Hughes, 2013; Hirabayashi et al., 2013; Winsemius et al., 2015; Alfieri et al., 2017, 2018; Kinoshita et al., 2018 *etc*). The expected intensification of floods may threaten the next generation and hamper effective socioeconomic development. Therefore, high-quality information on the global flood risk is required for effective socioeconomic development and adaption.

Modeling studies have projected river flood hazards, exposure, vulnerability, and risk at continental and global scales. Many of the global studies have dealt with the destruction of economic assets and infrastructure (referred to as "economic damage" hereafter). This is the total or partial destruction of physical assets in the affected area during and immediately after the flood (Jovel and Mudahar, 2010) (see Table 1). For example, Winsemius et al. (2015) projected that the absolute flood damage would

increase by the end of the century in South Asia due to climate change and in Africa due

to socioeconomic developments. Kinoshita et al. (2018) estimated a more than 8-fold

increase in potential economic damage until 2100 under the highest emission scenario

due to the large population increase.

Table 1. Definitions of the economic damage and losses caused by river flooding in this study.

Term	Definition	Example of components in this study
Economic damage	Total or partial destruction of physical assets in the affected area during and immediately after the flood (Jovel & Mudahar, 2010).	• Assets damage
Economic losses	Direct economic losses Temporary changes in the economic flow from the time of the flood until full economic recovery and reconstruction in the affected area (Jovel & Mudahar, 2010).	• Opportunity loss due to business interruption (BI loss) • Emergency measures costs
	Indirect economic losses Regional production reduction due to propagation to other sectors within the trade and supply network due to supply shortage, changes in demand, and associated price signals outside the flood-affected areas (Ciscar et al., 2011; Koks et al., 2015; Willner et al., 2018).	• Gross domestic product (GDP) losses

In addition to direct economic damage, floods with long inundation periods cause direct and indirect economic losses in and outside the affected area. The direct economic losses are temporary changes in the economic flow from the time of flooding until full economic recovery and reconstruction in the area (Jovel & Mudahar, 2010) (Table 1). Direct economic losses include opportunities losses due to business interruption (BI loss hereafter) and the cost of emergency measures (e.g., house rent and cleaning). Indirect economic losses are defined as the reduction in regional production due to propagation to other sectors within the trade and supply network due to supply shortage, changes in demand, and associated price signals outside the flood-affected areas (Ciscar et al., 2011; Koks et al., 2015; Willner et al., 2018). At local and regional scales, Koks et al. (2015) estimated the direct and indirect economic losses in the port region of Rotterdam, the Netherlands, using the Cobb–Douglas production function, which is based on the amount of production estimated using capital (the real value of all machinery, equipment, and building) and labor (the total number of person-hours worked) in each sector and using a hybrid input–output table. They found that direct economic losses were more significant than indirect economic losses, while the indirect economic losses were higher than the direct economic losses for low-probability flood events. Such estimation at continental and global scales is difficult due to the limited

availability of data on capital and labor for each sector. At continental and global scales,

the indirect economic losses have been estimated using a computable general

equilibrium (CGE) model (Ciscar et al., 2011; Dottori et al., 2018) or input–output

tables (Willner et al., 2018). For example, Dottori et al. (2018) estimated welfare losses

from river flooding using a CGE model and found that the welfare losses from river

flooding will increase with the increase in human losses and economic damage from

river flooding with global warming. These studies have contributed to understanding the

indirect economic losses from river flooding at large scales, however, there are still

limited studies to explicitly estimate other economic loss such as direct and indirect

economic losses induced by a long inundation period that halts operations in the

industry and manufacturing sectors because of limitation in modeling flood water depth

and inundation periods at finer scales.

We therefore developed a modeling framework to estimate direct (*i.e.,* BI loss

and emergency measures costs) and indirect (*i.e.,* gross domestic product (GDP) losses)

economic losses due to a flood with long inundation period using a CGE model forced

by a global river and inundation model, which is appropriately reproduced flood water

depth and inundation period at finer scales. The modeling framework is then applied to

the 2011 Thailand flood to examine how long-lasting inundation produce direct and

indirect economic losses, because the flood significantly affected the industrial sector

(*e.g.*, automotive and electronics industries) in Thailand (Haraguchi & Lall, 2015).

Finally, we discuss the potential application of the modeling framework on a global

scale. Such a modeling framework can capture a more complete picture of flood risk

and is important for effective socioeconomic development.

2. Methods

We developed a modeling framework to estimate the direct and indirect economic losses

caused by river flooding. In this study, the modeling framework was applied to the 2011

Thailand flood. The both economic losses were estimated as following stages (Figure

1):

i.   Calculation of daily total water storage using a global river and inundation

        model forced by a land surface model simulation;

ii.   Calculation of flood water depth, fraction of flooded area, and inundation

        period at 30″ × 30″ resolution from overflow flood water exceeding that

        corresponded to flood-protection standard from modeled total water storage;

iii.   Estimation of the direct economic losses and damage at 30″ × 30″ horizontal

resolution from the results of inundation calculation overlaying global

socioeconomic data;

iv.   Estimation of the indirect economic losses due to the related cross-sector

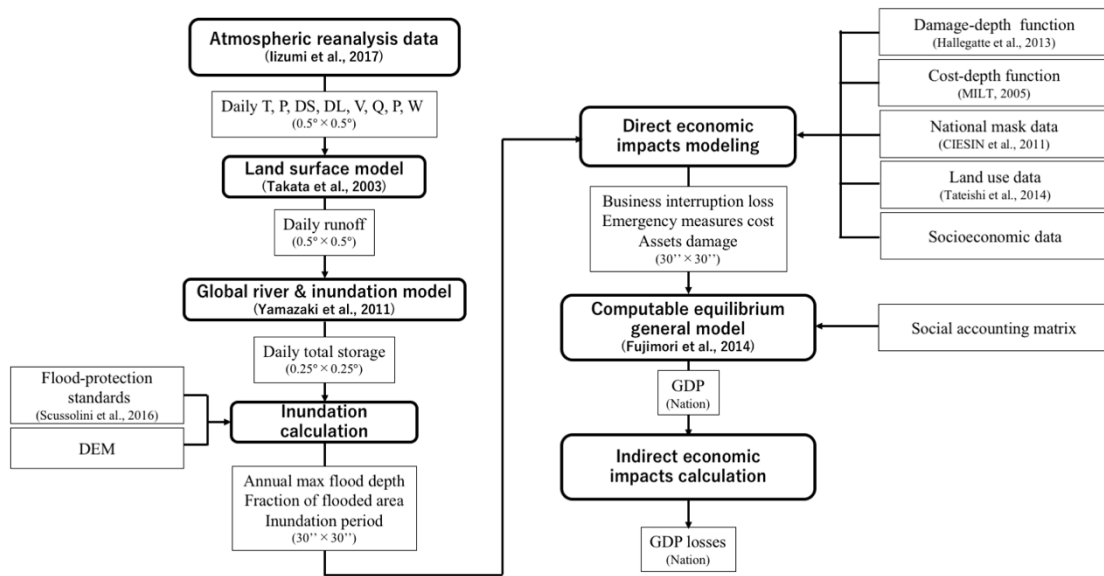second- and higher-order indirect economic effects using a CGE model.

Figure 1. Schematic illustration of a flow chart to estimate direct and indirect economic

losses.

2.1 Model

2.1.1 Land surface model

This study used the Minimal Advanced Treatments of Surface Integration and Runoff

model (MATSIRO) (Takata et al., 2003) to obtain daily runoff input to a global river

and inundation model simulation. MATSIRO is a land-surface process model with a

single-layer canopy and albedo that numerically simulates the land surface energy and

water fluxes at 0.5° × 0.5° horizontal resolution. MATSIRO calculates the vertical

energy and water fluxes in a grid cell based on soil properties and vegetation coverage

in both snow-free and snow-covered areas. Evapotranspiration is parameterized based

on photosynthesis (Sellers et al., 1996). Base flow, runoff, and surface flow are

computed from a simplified TOPMODEL (Beven & Kirkby, 1979). The model results

for the annual runoff were validated in Hirabayashi et al. (2005), who found that the

correlations between the simulated and observed annual runoff were high in many

basins, although they were low in dry and cold regions.

2.1.2 Global river and inundation model

The modeled total storage and river discharge at 0.25° × 0.25° horizontal resolution

were calculated using a global river and inundation model, the Catchment-based Macro-

scale Floodplain model (CaMa-Flood) (Yamazaki et al., 2011). CaMa-Flood integrated

the runoff input along a river network and calculated the river discharge, surface water

depth, flooded area, and total water storage volume at 0.25° × 0.25° resolution. The

water depth in the river channel and flooded area are obtained from the total water

storage. CaMa-Flood reasonably represented these river discharges in large river basins

(*e.g.,* Yamazaki et al., 2011; Hirabayashi et al., 2013; Ikeuchi et al., 2015; Tanoue et al.,

2016). The annual mean, annual maximum, and extreme values of river discharge have

been validated using observed river discharge at a continental scale (Hirabayashi et al.,

2013; Tanoue et al., 2016). Ikeuchi et al. (2015) described the time series of river

discharge and water depth in a flood plain in Bangladesh; CaMa-Flood represented the

variation and peaks well.

2.1.3 Computable general equilibrium model

The indirect impacts of the 2011 Thailand flood, including GDP changes, were

quantified using the Asia-Pacific Integrated model/Computable General Equilibrium

(AIM/CGE) model (Fujimori et al., 2014). The AIM/CGE model has been widely used

to assess climate change mitigation, development scenarios such as Shared

Socioeconomic Pathways (Fujimori et al., 2017), and associated impacts (Takakura et

al., 2018). In the CGE model, the production sectors are assumed to maximize profits

under multi-nested constant elasticity substitution (CES) functions for each input price.

Household expenditures for each commodity are described by a linear expenditure

system (LES) function. The parameters adopted in the LES function are updated

recursively using income elasticity assumptions. The savings ratio is determined

endogenously to balance savings and investment, and capital formation for each good is

determined by a fixed coefficient. The Armington assumption is used for trade (CES

and constant elasticity of transformation are assumed) and the current account is

assumed to be balanced.

2.2 Data

2.2.1 Atmospheric reanalysis data

We used the bias-corrected S14FD reanalysis dataset (Iizumi et al., 2017), which is

based on a Japanese 55-year reanalysis dataset corrected with observed climate

variables via spatial interpolation to a horizontal resolution of $0.5° \times 0.5°$ with elevation

corrections. S14FD contains global data for the period from 1958 to 2013 at 3-hour

intervals. The climatic variables include the 2-m air temperature, precipitation,

downward shortwave and longwave radiation fluxes, 2-m vapor pressure, specific,

relative, and absolute humidity, 10-m wind speed, and surface pressure. Daily values

were applied to make monthly-scale adjustments of the CRU-TS3.22 (air temperature,

vapor pressure, humidity, and wet days), CRU-CL1.0 (wind speed), NASA-POWER

(downward shortwave and longwave radiation), and GPCCv7 (precipitation)

observations. The corrections include the under-catchment of rain gauges under strong winds. Iizumi et al. (2017) compared the extreme temperature and precipitation indices derived from S14FD with those derived from other forcing data and found that S14FD frequently achieved better correspondence.

2.2.2 Flood-protection standards

To define the inundation by which the flood exceeded local flood protection measures (*e.g.*, levees and dams), we used the merged layer of the current flood-protection standards (FLOPROS) (Scussolini et al., 2016), which combines empirical information about existing flood-protection standards (design layer), information about flood-protection standards from policy regulations (policy layer), and estimates from the relationship between GDP and flood-protection standards (model layer). The FLOPROS polygon data were gridded to $0.25° \times 0.25°$ horizontal resolution. In most parts of Thailand, the model layer was applied with the values for 15 to 40 years, except for Bangkok, where a design layer with 50 years was applied, and Phuket, Phang Nga, Satun, and Narathiwat, which have no flood-protection standards.

2.2.3 Boundary data

For consistency with the socioeconomic data, we used national mask data derived from the Global Rural-Urban Mapping Project ver. 1 (GRUMPv1) (CIESIN et al., 2011). The horizontal resolution of GRUMPv1 is $30'' \times 30''$.

To estimate assets damage for urban regions, we used the current land-use data from the Global Land Cover by National Mapping Organizations (GLCNMO) ver. 2 (Tateishi et al., 2014). GLCNMO recognizes 20 categories and has a horizontal resolution of $15'' \times 15''$. We calculated the urban area fraction at $30'' \times 30''$ horizontal resolution from the GLCNMO data.

The global dataset of monthly irrigated and rain-fed crop areas around the year 2000 (MIRCA2000) (Portmann et al., 2010) was used to estimate the crop area exposed to river flooding. MIRCA2000 records the monthly crop area fraction at $5' \times 5'$ resolution worldwide. This study calculated and used the annual mean of the crop area fraction. Assuming a constant crop area fraction within a grid cell, we downscaled the annual mean of the crop area fraction to $30'' \times 30''$ horizontal resolution, and then multiplied it by the land surface area assuming a spherical ellipsoid.

2.2.4 Socioeconomic data

The population data was estimated by distributing the country population data from the

World Bank database (http://data.worldbank.org/ about/country-and-lending-groups)

using a population distribution map derived from the History Database of the Global

Environment (HYDE; ver. 3.1) in 2005 at $5' \times 5'$ horizontal resolution (Goldewijk et al.,

2011; Goldewijk & Verburg, 2013). The population was down-scaled using GRUMPv1

in 2000 (CIESIN et al., 2011) to $30'' \times 30''$ horizontal resolution.

The assets map was based on a combination of the population distribution map

at $30'' \times 30''$ horizontal resolution and year-basis GDP per capita data. We used the

GDP per capita in 2005 international US \$ on a PPP basis derived from James et al.

(2012); this dataset was a completed deflater using a PPP conversion factor for 215

countries for the period from 1960 to 2015. Population-based assets maps have been

widely used for global-scale flood risk assessments (e.g., Jongman et al., 2012 etc).

The number of households and office maps were based on a combination of the

population distribution map at $30'' \times 30''$ horizontal resolution and households and

office sizes per person. Because the numbers of households and offices sizes per person

are difficult to obtain globally, we used the numbers of households and offices in each

prefecture in Thailand derived from the Office of the National Economic and Social

Development Board (http://www.nesdb.go.th/nesdb_en/main.php?filename=index),

except for Chaiyaphum and Bueng Kan Provinces. The number of households used data

for 2010 and the number of offices used data for 2008. We calculated the mean

household and office sizes per person for each prefecture from these data. The mean

household and office sizes per person for prefectures in Thailand for which data were

available were applied for Chaiyaphum and Bueng Kan.

2.2.5 Satellite observation inundation map

An inundation map based on Terra/Moderate Resolution Imaging Spectroradiometer

(MODIS) images (Kotera et al., 2015) was used to validate the spatial distribution of the

inundation period. This study used inundation maps for 2011 at observation intervals of

8 days at 250 m horizontal resolution. Note that the inundation maps removed river

pixels when an inundation pixel appeared for more than 250 successive days to exclude

water surface in normal condition such as river and lake.

2.2.6 Disaster statics

The modeled total economic losses were compared with reported values (EM-DAT;

World Bank, 2012). The reported total economic losses have been given as a nominal

value. This was converted to a deflated PPP-based value (base year 2005) using the

ratio of the nominal total economic losses to the nominal GDP of Thailand in 2011

multiplied by the Thailand GDP on a PPP basis. Assets damage and direct economic

losses from the World Bank report (World Bank, 2012) were converted to PPP-based

values in the same way.

The dates that the inundation started and ended in seven industrial parks in

Thailand were obtained from a survey performed by the Japan External Trade

Organization (Sukegawa, 2012; Sukegawa 2013) to validate the modeled inundation

period (Table 2). Sukegawa (2012) and Sukegawa (2013) conducted surveys on 27

April, 1 June, and 1 October 2012, and reported the operation recovery rate defined as

the ratio of the total number of industries to the number of recovered industries in the

parks.

Table 2. The dates of the start and end of inundation in seven industrial parks in

Thailand.

Industrial park	Date inundation started	Date drainage completed	Operation recovery rate [%]		
			27 Apr. 2012	1 Jun. 2012	1 Oct. 2012
Rojana	9 Oct. 2011	28 Nov. 2011	64.8	72.3	77.9
Hi-tech	13 Oct. 2011	25 Nov. 2011	67.8	71.3	79.0
Factory Land	15 Oct. 2011	16 Nov. 2011	100.0	100.0	100.0
Banpa-in	14 Oct. 2011	17 Nov. 2011	82.2	85.6	87.8
Nava Nakorn	17 Oct. 2011	8 Dec. 2011	71.4	71.4	81.9
Saha Rattana Nakorn	4 Oct. 2011	4 Dec. 2011	56.5	58.7	58.7
Bankadi	20 Oct. 2011	4 Dec. 2011	66.7	66.7	80.6

Source: Sukegawa (2012) and Sukegawa (2013)

2.3 Estimation of economic losses and damage

2.3.1 BI loss

The BI loss was estimated as the reduction in industrial production. Figure 2 shows a

schematic illustration of BI loss. We assume that production values were zero during the

inundation period and then recovered linearly, since most industries and manufactures

cannot immediately start production and require a start-up time, referred to as the

"preparation period" below. The production amount per day is assumed to be not vary in

a year. BI loss ($Loss_{BI}$) due to inundation can be estimated by the following equation:

$$Loss_{BI} = \left(D_{flood} + \frac{D_{prep}}{2} \right) \times P$$

where *P* is the daily production value (US $/day), and D_{flood} and D_{prep} are the numbers

of days of flood inundation and preparation period after river flooding (day),

respectively. *P* was obtained by multiplying assets by the ratio of the production in the

industry and service sectors by the total GDP in 2010 derived from the World Bank

database. The value is 0.895 in the case of Thailand. Figure 3 shows the relationship

between the ratios of the preparation to the inundation period (α) and the operation

recovery rate of the industrial park in Bangkok, Thailand affected by the 2011 Thailand

flood. The two were highly correlated (R = 0.77, $p < 0.01$). Because extending the

regression line to 100% of operation recovery rate derived $a = 11.50$, we estimated as
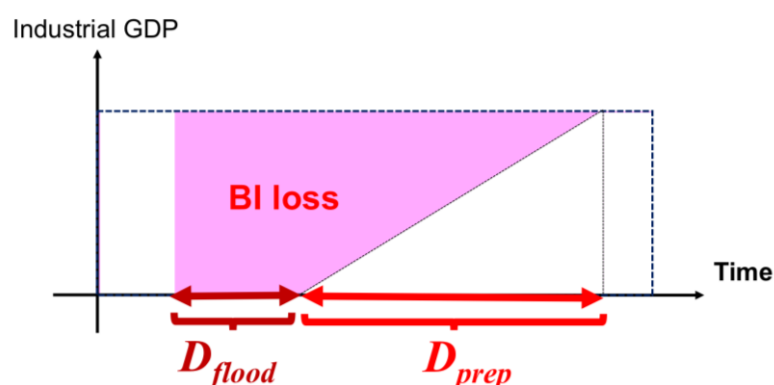
$$D_{prep} = 11.50 \times D_{flood}.$$

Figure 2. Schematic illustration of the calculation of BI loss in this study. D_{flood} and

D_{prep} are the inundation period during the flooding and preparation periods for operation

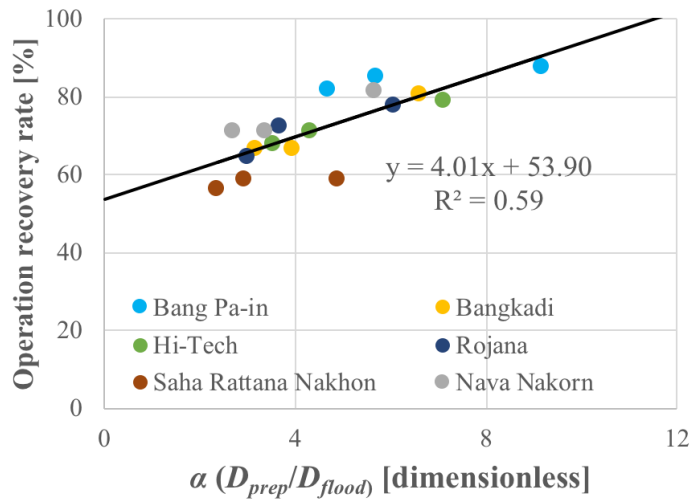recovery after the flood, respectively.

Figure 3. Relationship between the operation recovery rate and the ratio of preparation period to inundation period in industrial parks in Thailand. The black solid line is the regression line.

2.3.2 Emergency measures costs

The emergency measures costs include the cost of house cleaning, alternative housing expenditures, and emergency expenditures associated with alternative activities.

The house cleaning costs are the expenses required for cleaning labor in the household sector and are calculated using the following equation:

$$Loss_{Clean} = N_{house} \times D_{clean} \times C_{clean}$$

where $Loss_{Clean}$ is the house cleaning cost (US \$), N_{house} is the number of households (household), D_{clean} is the number of days of cleaning extension (days), and C_{clean} is the

value of labor (US $/day/household). We assumed D_{clean} to be a function of the annual

maximum flood water depth, because house cleaning is required when a house is

inundated, regardless of the inundation period. D_{clean} was determined from statistics for

past flood disasters in Japan based on questionnaire surveys of water-related disasters in

2005 and 2006 (MLIT, 2005) (Table 3). C_{clean} was derived from *MLIT* [2005], which

was calculated from the daily wage of port cargo handlers and building cleaners. C_{clean}

was described in current local currency (¥10,360 in 2003) and converted to a deflated,

PPP-based value ($8.1 PPP, base year 2005). This value (approximately 247 THB) is

close to the minimum daily wage in Thailand (300–310 THB, Ministry of Labor).

Table 3. Summary of the number of days of house cleaning as a function of flood water

depth.

Flood water depth [m]	D_{clean} [days]
0.50–0.99	13.3
1.00–1.99	26.1
2.00–2.99	42.4
> 3.00	50.1

Alternative housing expenses are needed when residents are evacuated. We

assumed that house retortion and lifeline are recovered from inundation to the end of

house cleaning. Alternative housing expenses were estimated with the following

equation:

$$Loss_{AHE} = (D_{flood} + D_{clean}) \times N_{house} \times C_{house}$$

where C_{house} is the housing consumption (US \$/household/day). Assuming that income

and its share of housing consumption are the same in a country, then C_{house} can be

estimated with the following equation:

$$C_{house} = GCAP_{day} \times S_{house} \times R_{house}$$

where $GCAP_{day}$ is the GDP per capita per day (US \$/person/day), S_{house} is the mean

household size (person/household), and R_{house} is the share of housing consumption to

income (dimensionless). R_{house} was obtained from the World Bank Global Consumption

Database (http://datatopics.worldbank.org/consumption/country/). For Thailand, R_{house}

was set to 29.38%.

Emergency expenditure costs associated with alternative activities include the

purchase of drinking water and commuting expenses. Emergency expenditure costs

($Loss_{EEC}$) were estimated for the household and office sectors using the following

equation:

$$Loss_{EEC} = N_{house} \times EB_{house} + N_{office} \times EB_{office}$$

where N_{office} is the number of offices, and EB_{house} and EB_{office} are the alternative activity

expenditure burden unit prices in the household and office sectors, respectively. EB_{house}

and EB_{office} are a function as the annual maximum flood water depth (Table 4). EB_{house}

and EB_{office} were obtained from MLIT (2005) in current local currency in 2003. These

values were calculated based on surveys of flood damage and losses in Japan that

occurred in 2005 and 2006. To consider the difference in price and deflater between

Japan and Thailand, EB_{house} and EB_{office} were deflated and converted to PPP values in

the same manner as the conversion of C_{house}.

Table 4. Alternative activity expenditure unit price in the household and business

sectors.

Flood water depth [m]	EB_{house} [US $ PPP (base year 2005)/household]	EB_{office} [US $ PPP (base year 2005)/office]
0.50–0.99	158	1,315
1.00–1.99	212	2,859
2.00–2.99	250	5,030
> 3.00	263	5,078

2.3.3 Assets damage

Assets damage caused by river floods was calculated using the modeled flood water depth, fraction of flooded area, capital stock, and damage–depth functions. We used the damage–depth function of Huizinga et al. (2017) for each region (Asia, Africa, Europe, Oceania, North America, and Central & South America), which was estimated using functions based on a literature survey. Table 5 showed the example of the damage–depth function for Asia. A map of capital stock was created by multiplying the assets map by a stock conversion coefficient. In this study, we applied a coefficient of 2.8 for a grid with urban land use (Hallegatte et al., 2013), which was estimated from the relationship between GDP per capita and capital produced per capita using the World Bank dataset. For the other region, a coefficient of 1.0 was applied (Alfieri et al., 2015).

Table 5. Damage–depth function in the Asia region.

Flood water depth [m]	Damage ratio [dimensionless]
0.0–0.50	0.000
0.50–0.99	0.312
1.00–1.49	0.492
1.50–1.99	0.648
2.00–2.99	0.752
3.00–3.99	0.884
4.00–4.99	0.934
5.00–5.99	0.978
> 6.00	1.000

2.3.4 Indirect economic losses

To input the modeled assets damage and direct economic losses into the AIM/CGE

model, we first aggregated the assets damage and direct economic losses to national and

annual scales, and then calculated the damage ratio to capital stock, the rate of reduction

of capital mobility, additional expenditures, and the rate of reduction of farmland use.

The damage ratio to capital stock was calculated as the total of the modeled assets

damage divided by the total capital stock in the production sector when flood event

occurred. The rate of reduction of capital mobility in the four departments was

calculated as the total BI loss divided by the annual total production in all sectors in the

same year. The additional expenditures in the household and business sectors were same

as the total values of the emergency measures costs in the household and business

sectors. The rate of reduction in farmland use was estimated as the total inundated crop

area divided by the total crop area in Thailand. We assumed that farmland that was

inundated for more than 30 days could not produce crops; the total inundated crop area

was calculated from the total farmland.

2.4 Experiment design

2.4.1 Simulation

Daily runoff at 0.5° × 0.5° resolution was simulated by the land surface model

MATSIRO (Takata et al., 2003) forced by atmospheric forcing data from S14FD (Iizumi

et al., 2017) from 1958 to 2013 at 3-hour intervals. The CaMa-Flood (Yamazaki et al.,

2011) simulation was forced by the daily runoff and output daily total storage at 0.25° ×

0.25° resolution for the period 1958–2013.

2.4.2 Inundation calculation

To reflect the effects of current flood-protection standards, we calculated the overflow

flood water depth at 0.25° × 0.25° resolution from the modeled daily total storage and

total storage corresponding to current flood-protection standards obtained from

FLOPROS. Inundation was calculated only when the total water storage exceeded that

equivalent to the current flood-protection standards. It was calculated using the Gumbel

distribution using L-moment methods from the annual maximum total storage for the

period 1961–2005.

The overflow flood water depth was downscaled to 30″ × 30″ horizontal resolution (approximately 1 km × 1 km at the equator) using a high-resolution digital elevation model. The flooded area fraction was calculated at the same resolution.

The inundation period is defined as the continuous period between the start and end of inundation. The start of inundation is defined as the time when the overflow flood water depth exceeded 0 m, and the end of inundation is defined as the time when the overflow flood water depth was below h m after the peak. We assumed self-protection by local people and industries against river flooding, and h was set to 1.0 m. The inundation period was calculated at 30″ × 30″ resolution. If there were more than two inundations in a year, we selected the maximum inundation period of the two. Because the annual maximum river discharge in most downstream cells occurs in September or November in northern hemisphere, we defined the hydrological year as running from July to June and calculated the inundation period for the hydrological year (*i.e.*, from July 2011 to June 2012).

2.4.3 Direct economic losses and damage

The direct economic losses and damage were calculated for the hydrological year (*i.e.*, from July 2011 to June 2012) at $30'' \times 30''$ resolution. Population and assets maps in 2011 were used for the calculation.

2.4.4 Estimation of GDP losses

The indirect economic losses were calculated until 2030 using the social accounting matrix of a country affected by flood. The data in 2005 was used for the case of 201 Thailand flood. Future GDP change was obtained from Shared Socioeconomic Pathway 2 (middle of the road). We assumed that the rebound effect of flood economic losses due to international trade and price changes was small, and so international trade is not considered in this analysis. A capital stock was created based on the value of capital formation from the World Bank; a 4% annual rate of creating capital stock was used in this application. Damaged capital stock was recovered by capital formation; it was estimated from the assets damage multiplied by 0.66, which was based on a report about the 2011 Thailand flood (World Bank, 2012). The AIM/CGE model calculated GDP in the cases of occurrence and no-occurrence of flood impacts using the social accounting

Water Resources Research

matrix. GDP losses were quantified as the difference in the GDP with and without the

effects of economic flood impacts.

2.4.5 Sensitivity analysis

To assess the sensitivity of the total of direct economic losses and damage to the flood-

protection standards, we calculated these assuming various flood-protection standards.

Overflow flood water depth at 0.25° × 0.25° resolution was calculated using constant

flood-protection standards (2-, 5-, 10-, 20-, 50-, and 100-year return periods), and then

downscaled to 30″ × 30″ resolution. Finally, the direct economic losses and damage

using the constant flood-protection standards were calculated.

3. Results

3.1 Validation of the reanalysis river flood simulation

The daily river discharge derived from the Global Runoff Data Center was used to

check the variation and peaks in the simulated river discharge (Figure 4). The validation

was conducted at the Khai Chira Prawat (100.67°E, 15.67°N) and What Pho Ngam Ban

Re Rai (100.19°E, 15.17°N) stations for the period 1990–1999. Figure 4 shows the

correlation coefficient, probability, and root mean square error (RMSE) between the

observed and simulated values. Given the significant ($p < 0.01$) correlations at both

observation sites, the model captured the seasonal and annual variation and peaks in

river discharge. However, the RMSE was high at both stations (597 m³/s for Khai Chira

Prawat and 761 m³/s for What Pho Ngam Re Rai) due to the delayed peak in river

discharge in the simulation. Moreover, the model underestimated the low river

discharge from January to March. These discrepancies arise from the uncertainty of the

precipitation field from S14FD, that of the runoff field simulated by MATSIRO, and the

human modification of river discharge (*e.g.*, withdrawal of water, dam operations, etc.).
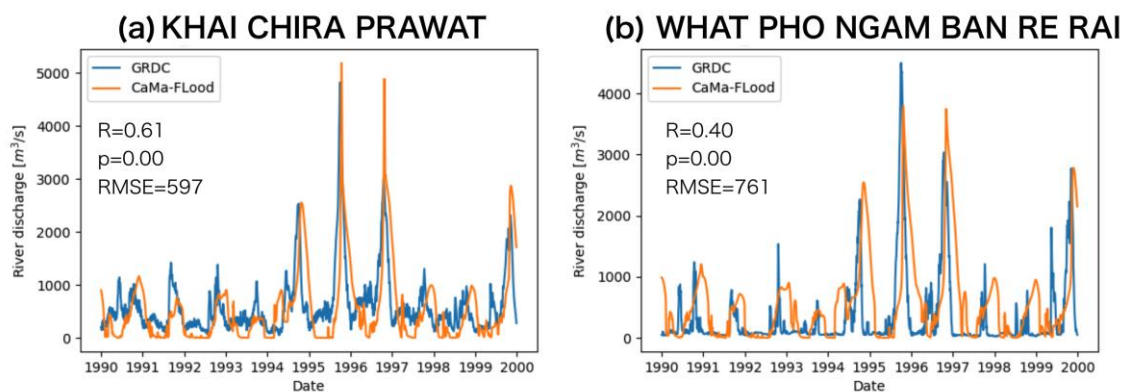
Figure 4. Daily variation in river discharge derived from the global runoff data center

(GRDC) and a global river and inundation model (CaMa-Flood) at the (a) Khai Chira

Prawat (100.67°E, 15.67°N) and (b) What Pho Ngam Ban Re Rai (100.19°E, 15.17°N)

stations for the period 1990–1999. The correlation coefficient (R), probability (p), and

root mean square error (RMSE) between GRDC and CaMa-Flood are also shown.

The modeled inundation period used to calculate the BI loss was validated

against that estimated from MODIS images and the reported inundation period. The

inundation period from the MODIS images exceed 100 days at the confluence of the

Nan and Ping Rivers and in the region between the Chao Phraya and Tha Chin Rivers

(Figure 5a). Figure 5b shows the spatial distribution of the modeled inundation period.

The simulation reproduced the long inundation periods in the confluence region and

downstream region of the Chao Playa River. However, the model simulation also found

a long inundation period downstream at the Bhumibol and Sirikit Dams (not shown in

Figure 5a). The overestimation of the modeled inundation period was found by a

comparison with reports for the Hi-tech, Banpa-in, and Saha Rattana Nakorn Industrial

Parks (Figure 6). The modeled inundation period was 23–42 days longer than the

reported values. The start of inundation in the model simulation was close to the

reported values, while the end of inundation was late compared with the reported

values, despite assuming self-flood protection (*i.e.*, $h = 1.0$ m). These overestimations of

the modeled inundation period led to overestimation of the BI loss. One plausible

reason for this discrepancy is because CaMa-Flood does not assume the reservoir

operation by Bhumibol and Sirikit Dams, while previous study indicated that these

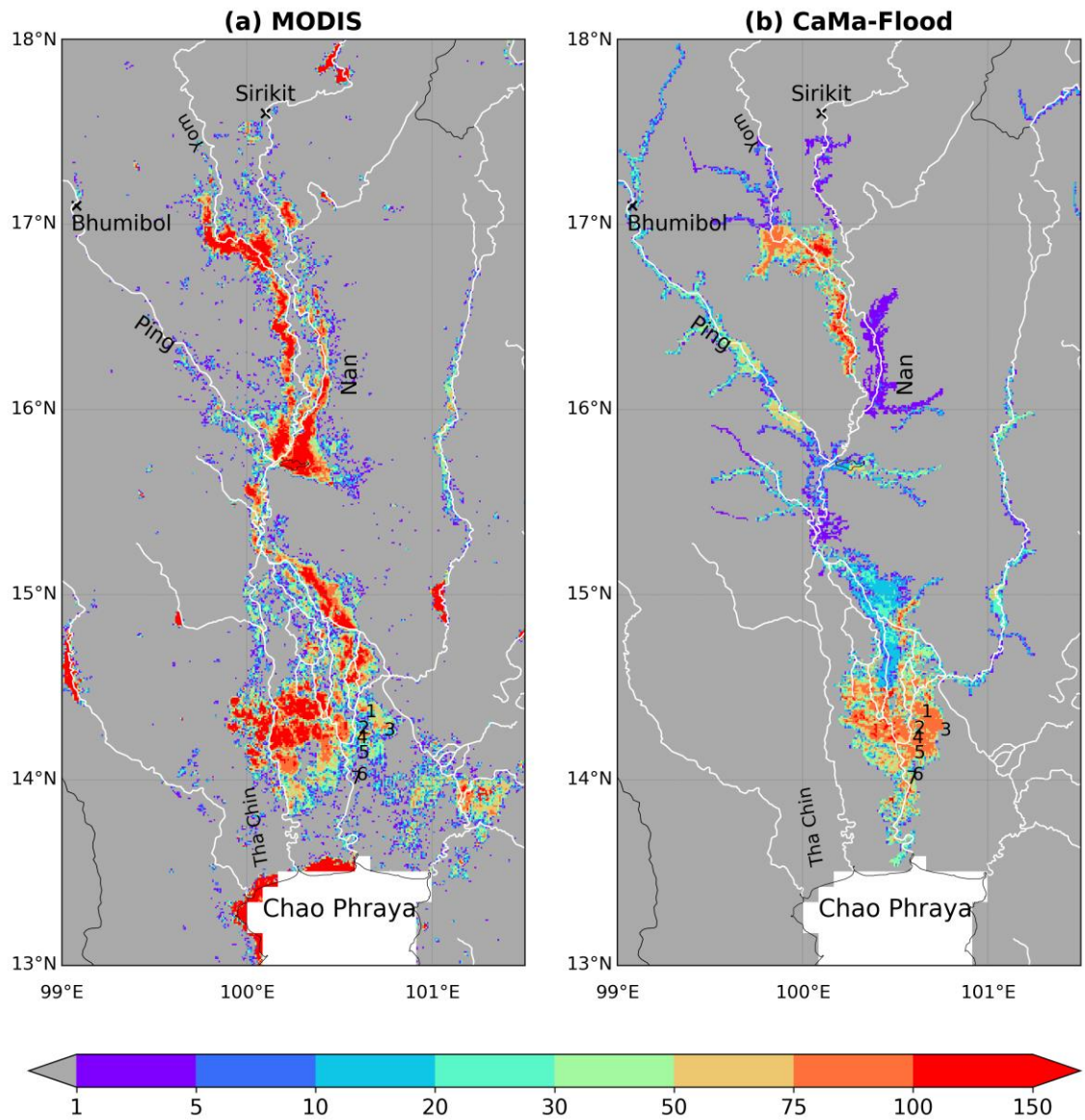dams stored about half of the floodwater during the flood event (Komori et al., 2012).

Figure 5. Spatial distribution of the inundation period [days] derived from (a) MODIS

images and (b) the CaMa-Flood simulation. White and black solid lines indicated rivers

and national boundaries, respectively. Black crosses indicate the locations of large

reservoirs in the basin. The numbers are the locations of the 1) Rojana, 2) Hi-tech,

3) Factory Land, 4) Banpa-in, 5) Nava Nakorn, 6) Saha Rattana Nakorn, and 7) Bankadi
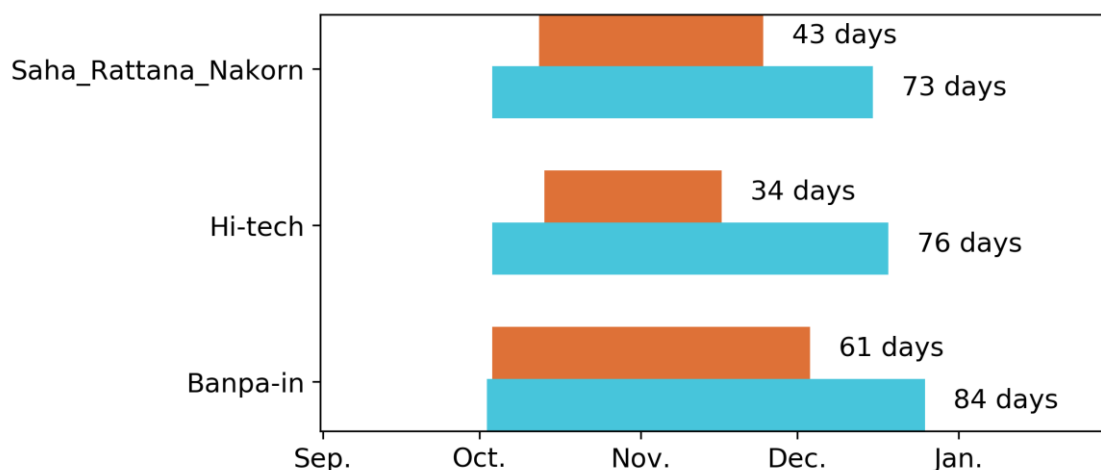
Industrial Parks.

Figure 6. Validation of the modeled inundation period against the reported inundation

period for the Hi-tech, Saha Rattana Nakorn, and Banpa-in Industrial Parks. The brown

and blue boxes indicated the reported and modeled inundation periods, respectively.

3.2 Direct and indirect economic losses

Direct economic losses and assets damage exceeded $10 million PPP in the downstream

region of the Chao Playa River, in particularly to the west of the river (Figure 7). Direct

economic losses and assets damage were low near the Ping, Yom, and Nan Rivers,

because there are few assets in the region. The spatial pattern of direct economic losses

was similar to that of assets damage; assets damage exceeded direct economic losses
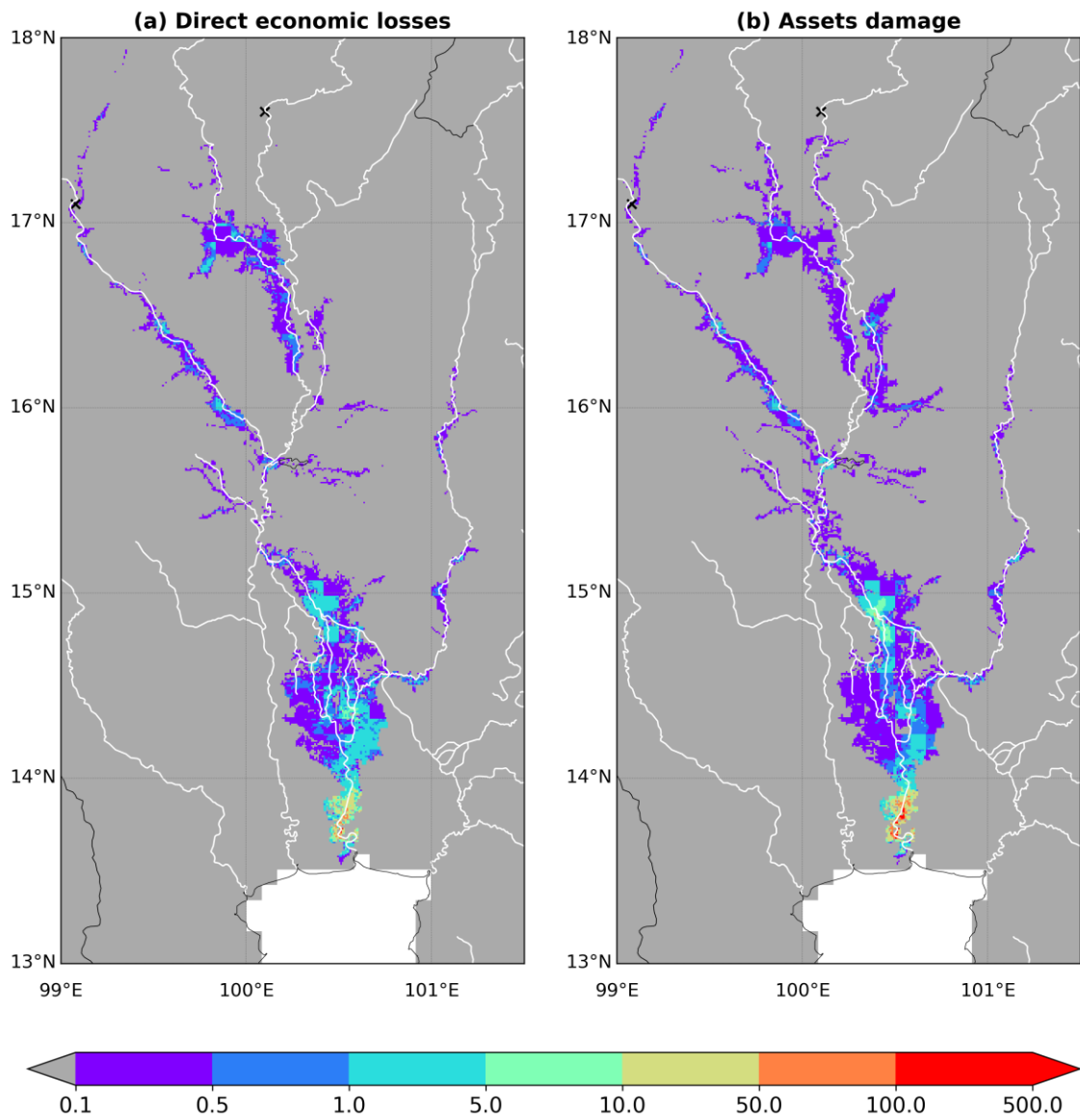
near Bangkok.

Figure 7. Spatial distributions of the simulated (a) direct economic losses and (b) assets

damage. The units of the direct economic losses and assets damage are US $1 million

PPP (base year 2005).

The assets damage and direct economic losses totaled US $36.7 billion PPP

(base year 2005) (Table 6). Direct economic losses ($14.7 billion PPP) were calculated

from the BI loss ($12.1 billion PPP) and emergency measures costs ($2.6 billion PPP)

and contributed 40.0% of the total. The direct economic losses were equivalent in

magnitude to the assets damage ($22.0 billion PPP). Emergency measures costs were

calculated from house cleaning ($0.5 billion), house rent ($1.2 billion), and emergency

measures costs in the household ($0.4 billion) and office ($0.5 billion) sectors. These

components were one order of magnitude smaller than the BI loss.

Table 6. Summary of indirect economic losses due to direct economic losses and assets

damage.

	Model simulation [billion US$]	GDP losses (2011) [billion US$]	GDP losses (2011- 2030) [billion US$]
Direct economic losses	14.7	6.2	6.2
BI loss	12.1	6.0	6.0
Emergency measures cost	2.6	0.2	0.2
Assets damage	22.0	4.4	49.2

The GDP losses due to spillover effects to other sectors within the trade and

supply network due to the 2011 Thailand flood reached 5.48% ($10.4 billion PPP). This

is equivalent in magnitude to a quarter of the total assets damage and direct economic

losses (Figure 8). Assets damage to production capital stock (2.04%) and a reduction in

capital mobility due to business interruption in the department (2.77%) were dominant

factors in the GDP losses. Note that the reduction in capital mobility was stronger

because of indirect effects through the trade and supply chain than direct damage to

capital stock, although the BI loss ($14.7 billion PPP) was lower than the assets damage

($22.0 billion PPP). In comparison, the additional expenditure in the household and

office sectors (0.05%) and the reduction in farmland use due to prolonged inundation

(0.05%) were minor factors in the GDP losses. The effects to other sectors of these

losses were small within the trade and supply network. These economic impacts were

reduced to 5.07% of the economic gross in 2011 (the difference between 5.48% without

flood impacts and 0.41% with flood impacts). The reduction in the economic growth

rate due to BI loss (2.92%) was higher than that due to assets damage (2.15%). The

impact of BI losses on the economy and its growth was stronger than that of assets

damage due to spillover effects to other sectors via the trade and supply network.

Interestingly, a reduction in GDP was observed after the flood event, as well as

during the event. The GDP losses after the flood event were due to damage to capital

stock, which will reduce the GDP by more than 0.5% annually until 2030. The total

GDP losses from 2012 to 2030 reached $42.8 billion PPP with a 5% discount rate. This

exceeds the total GDP losses in 2011 ($10.6 billion PPP). In our estimation, the indirect

economic losses from 2011 to 2030 totaled $55.3 billion PPP. Damage to capital stock

reduced production in the affected departments, causing indirect long-term economic

losses in the country due to propagation to other sectors within the trade and supply

network. This shows that the flood will inhibit socioeconomic development for a long
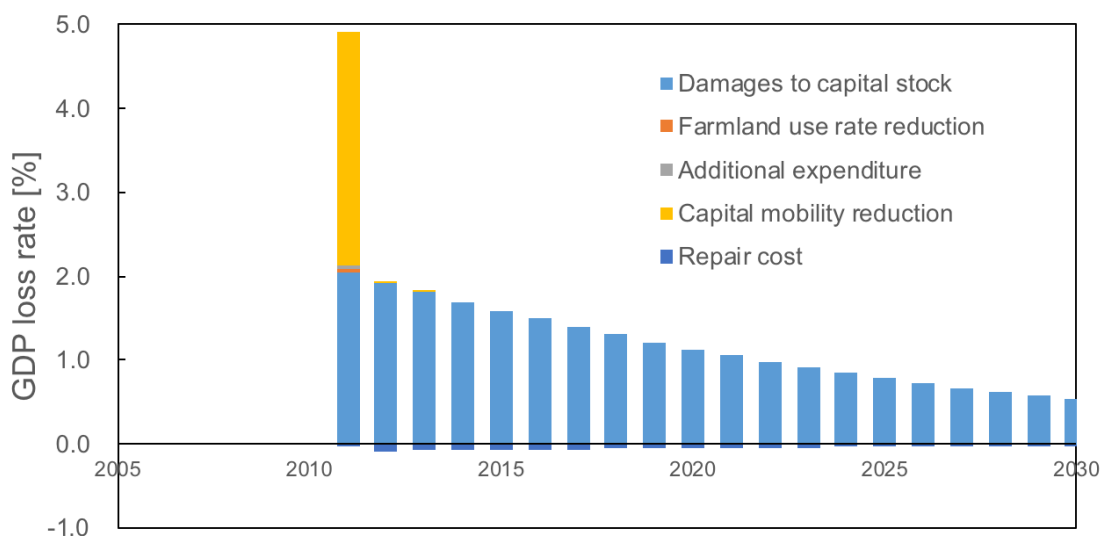
time after the flood.

Figure 8. Annual variation in the GDP loss rate due to the effects of the damage to

capital stocks, reduced farmland use, reduced capital mobility, additional expenditures,

and repair costs.

4. Discussion

The estimated total of direct economic losses and damage ($36.7 billion PPP) was higher than the reported values derived from EM-DAT ($22.9 billion PPP) and World Bank (2012) ($21.0 billion PPP). These overestimations were due to the effect of flood water storage by the Bhumibol and Sirikit Dams, because these dams stored half of the flood water during the flood (Komori et al., 2012), resulting in a reduction in the annual maximum flood water depth and inundation period downstream in the Chao Playa River basin. A sensitivity simulation using 50% reduction of runoff input from the upper basin of the dams showed that the overestimation of the modeled inundation period in the industrial parks decreased to less than 10 days (not shown) and resulted lower direct economic losses and assets damages ($7.6 and $12.5 billion PPP (base year 2005), respectively).

Other potential source of the uncertainty is flood-protection standard implemented in the model. Here, we analyzed the sensitivity of the total economic losses and its ratio of direct economic losses to the flood-protection standards (Figure 9). This showed that enhanced flood-protection standards significantly reduced the total assets damage and direct economic losses. The total ranged from $20.7 to $65.4 billion assuming 2- to 100-

year return periods as flood-protection standards. Moreover, the ratio of direct economic

losses to the total was reduced by enhancing the flood-protection standards (from 65.4%

to 20.7%). These results suggest that direct economic losses affect regions with low

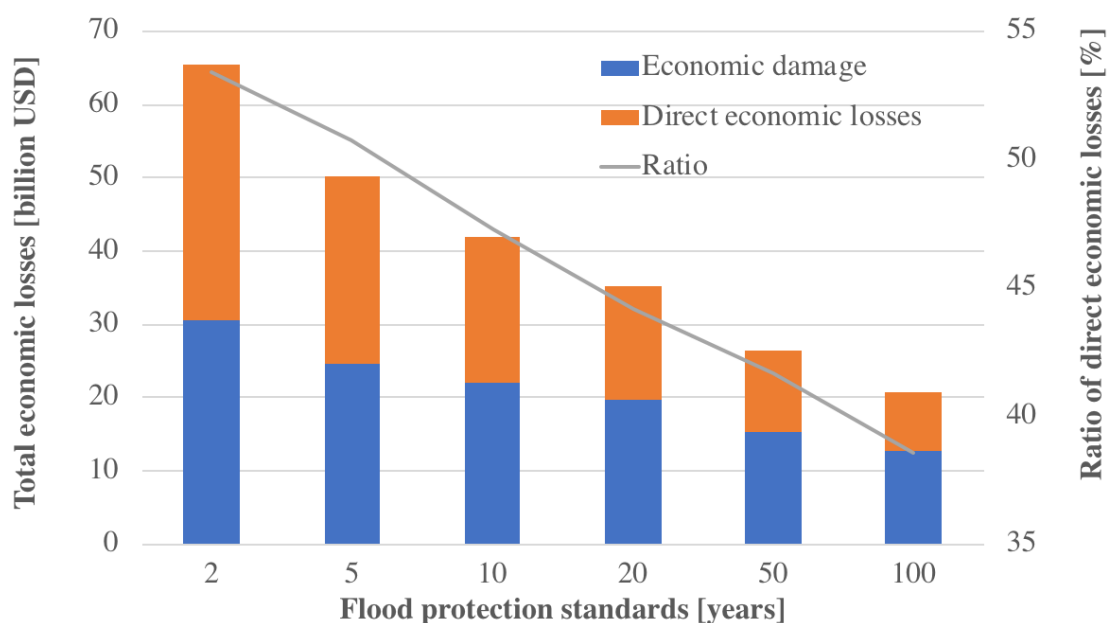flood-protection standards more strongly, such as low-income countries.

Figure 9. Sensitivity analysis of total economic losses to flood-protection standards.

Our results showed that flood economic losses and damage have short- and long-

term socioeconomic effects. In particular, BI losses induce a reduction in capital

mobility, resulting in a strong GDP reduction due to spillover effects to other sectors.

By contrast, damage to production capital stock reduced the production capacity in each

production sector after the flood, resulting in long-term GDP reduction. Some points

regarding the interpretation of the results must be noted. First, this framework did not

consider international trade because of the assumption of a small rebound effect of flood

economic losses due to international trade and price changes. However, this flood event

affected a wide region due to spillover effects to other sectors, resulting in price changes

of products in the manufacturing sector (Haraguchi & Lall, 2015). Therefore,

international trade must be considered to estimate the indirect economic losses due to

the 2011 Thailand flood in other countries and regions. Second, the input–output table

for 2005 was used, *i.e.*, before the flood. This implicitly assumes that the industrial

structure is similar to the base year situation, although there were drastic structural

changes due to the flood and innovative technology. Changes in the industrial structure

might or might not change the scale of the GDP losses in Thailand (Willner et al.,

2018).

There is room to improve the modeling of the inundation period and estimating

the direct economic losses and damage. For example, the modeled inundation period in

the region downstream from the Bhumibol and Sirikit Dams was overestimated,

because CaMa-Flood does not assume human modifications of river discharge. Human

modifications, such as dam operations and the removal of water from the river, should

be considered for high-quality modeling of the inundation period. Mateo et al. (2014)

incorporated such human modifications of river discharge into CaMa-Flood and showed

that this increased the accuracy of river discharge modeling. The estimation of BI loss is

sensitive to the rates of operation recovery and the inundation period to the preparation

period (α); these ratios must be improved to obtain high-quality flood-risk information,

as it reflects hazards, culture, disaster experiences, vulnerability, mitigation measures,

and national and political differences. Although this study assumed a 100% operation

recovery rate, Sukegawa (2012) and Sukegawa (2013) reported that 10% of the

businesses in the industrial parks closed because of the flood. The assumed full

recovery of operations was likely an overestimation.

We developed a modeling framework that can be applied to global-scale

assessments, based on a global river and inundation model, a global socioeconomics

dataset, a CGE model and globally available climate dataset. A uniqueness of our

methodology is utilization of a bias-corrected climate dataset that allow us to use

absolute value of modeled flood water depth to calculate inundation period. Many of the

earlier flood-risk studies have used the statistical runoff change derived from GCM

simulations (Hirabayashi et al., 2013) to estimate flood damage and losses using a

method such as look-up table between return period and flood water depth, because an

absolute value of river discharge and hence flood water depths in GCM simulations

contain model biases. This is one of the reason that there are limited studies to estimate

direct economic losses such as business interruption requiring adequate modeling of

inundation period.

5. Summary

We developed a modeling framework to estimate direct (*i.e.,* BI losses and emergency

measures cost) and indirect economic losses (*i.e.,* GDP losses) due to a flood with long

inundation period using AIM/CGE model forced by CaMa-Flood, which was

appropriately reproduced flood water depth and inundation period. We applied the

modeling framework for the 2011 Thailand flood, the estimated direct economic losses

amounted to $14.7 billion on a PPP basis, these were equivalent in magnitude to the

assets damage ($22.0 billion PPP). The indirect economic losses caused by the flooding

were occurred for short- and long-term periods after flooding. The GDP losses for short-

term period were mainly derived from business interruption losses (*i.e.,* BI losses) and

destruction of physical assets (*i.e.,* assets damage), while those for long-term period

were caused by assets damage. In our estimation, the total GDP losses from 2011 to

2030 reached $55.3 billion, with a 5% discount rate, those were higher than the total

economic losses in 2011. Our modeling framework could help us to understand various

types of flood risk on economy for short- and long-term period after flooding. Because

the modeling framework based on global scale models and dataset, this could be

applicable to estimate indirect economic losses due to a flood at global and continental

scales.

Acknowledgments and Data

References

Alfieri, L., Feyen, L., Dottori, F., & Bianchi, A. (2015), Ensemble flood risk assessment in Europe under high end climate scenarios. *Global Environmental Change*, 35, 199-212, doi: 10.1016/j.gloenvcha.2015.09.004.

Alfieri, L., Bisselink, B., Dottori, F., Naumann, G., Roo, A. d., Salamon, P., Wyser, K., et al. (2017). Global projections of river flood risk in a warmer world. *Earth's Future*, *5*(2), 171-182, doi: 10.1002/2016ef000485.

Alfieri, L., Dottori, F., Betts, R., Salamon, P., & Feyen, L. (2018). Multi-Model Projections of River Flood Risk in Europe under Global Warming. *Climate*, *6*(1), doi: 10.3390/cli6010006.

Arnell, N. W., & Lloyd-Hughes, B. (2013). The global-scale impacts of climate change on water resources and flooding under new climate and socio-economic scenarios. *Climatic Change*, *122*(1-2), 127-140, doi: 10.1007/s10584-013-0948-4.

Beven, K. J., & Kirkby, M. J. (1979). A physically based, variable contributing area model of basin hydrology. *Hydrological Sciences Bulletin*, *24*(1), 43-69, doi: 10.1080/02626667909491834.

Ciscar, J. C., Iglesias, A., Feyen, L., Szabó, L., Regemorter, D. V., Amelung, B, Nicholls, R. et al. (2011). Physical and economic consequences of climate change in

Europe. *Proceedings of the National Academy of Sciences of the United States of America*, *108*(7), 2678-2683, doi: 10.1073/pnas.1011612108.

Dottori, F., Szewczyk, W., Ciscar, J. C., Zhao, F., Alfieri, L., Hirabayashi, Y., Bianchi, A. et al. (2018). Increased human and economic losses from river flooding with anthropogenic warming. *Nature Climate Change*, *8*(9), 781-786, doi: 10.1038/s41558-018-0257-z.

Center for International Earth Science Information Network (CIESIN), Columbia University; International Food Policy Research Institute (IFPRI); the World Bank; and Centro Internacional de Agricultura Tropical (CIAT) (2011), Global Rural-Urban Mapping Project, Version 1 (GRUMPv1): Population Count Grid. Palisades, NY: Socioeconomic Data and Applications Center (SEDAC), Columbia University. Available at http://sedac.ciesin.columbia.edu/data/dataset/grump-v1-population-count. (Access Accessed 17 January 2019).

EM-DAT: The OFDA/CRED international disaster database, University Catholic Louvain-Brussels, Belgium. Available at www.emdat.be. (Access Accessed 17 January 2019).

Fujimori, S., Masui, T. & Matsuoka, Y. (2014). Development of a global computable

general equilibrium model coupled with detailed energy end-use technology.

Applied Energy, *128*, 296-306, doi: 10.1016/j.apenergy.2014.04.074.

Fujimori, S., Hasegawa, T., Masui, T., Takahashi, K., Herran, D. S., Dai, H., Hijioka, Y.,

& Kainuma, M. (2017). SSP3: AIM implementation of Shared Socioeconomic

Pathways. *Global Environmental Change*, *42*, 268-283, doi:

10.1016/j.gloenvcha.2016.06.009.

Hallegatte, S., Green, C., Nicholls, R. J., & Corfee-Morlot, J. (2013). Future flood

losses in major coastal cities. *Nature Climate Change*, *3*, 802-806, doi:

10.1038/nclimate1979.

Hanasaki, N., Kanae, S., & Oki, T. (2006). A reservoir operation scheme for global river

routing models. *Journal of Hydrology*, *327*(1-2), 22-41, doi:

10.1016/j.jhydrol.2005.11.011.

Hanasaki, N., Kanae, S., Oki, T., Masuda, K., Motoya, K., Shirakawa, N., Shen, Y., &

Tanaka, K. (2008). An integrated model for the assessment of global water resources

Part 1: Model description and input meteorological forcing. *Hydrology and Earth*

System Sciences, *12*(4), 1007-1025, doi: DOI 10.5194/hess-12-1007-2008.

Haraguchi, M., & Lall, U. (2015). Flood risks and impacts: A case study of Thailand's

floods in 2011 and research questions for supply chain decision making.

International Journal of Disaster Risk Reduction, *14*, 256-272, doi:

10.1016/j.ijdrr.2014.09.005.

Hirabayashi, Y., Kanae, S., Struthers, I., & Oki, T. (2005). A 100-year (1901-2000)

global retrospective estimation of the terrestrial water cycle. *Journal of Geophysical*

Research-Atmospheres, *110*(D19), doi: 10.1029/2004jd005492.

Hirabayashi, Y., Mahendran, R., Koirala, S., Konoshima, L., Yamazaki, D., Watanabe,

S., Kim, H., & Kanae, S. (2013). Global flood risk under climate change. *Nature*

Climate Change, *3*(9), 816-821, doi: 10.1038/nclimate1911.

Huizinga, J., Moel, H. d., & Szewczyk, W. (2017). Global flood depth-damage

functions: Methodology and the database with guidelines. EUR 28552 EN. doi:

10.2760/16510.

Iizumi, T., Takikawa, H., Hirabayashi, Y., Hanasaki, N., & Nishimori, M. (2017).

Contributions of different bias-correction methods and reference meteorological

forcing data sets to uncertainty in projected temperature and precipitation extremes.

Journal of Geophysical Research: Atmospheres, *122*(15), 7800-7819, doi:

10.1002/2017jd026613.

Ikeuchi, H., Hirabayashi, Y., Yamazaki, D., Kiguchi, M., Koirala, S., Nagano, T.,

Kotera, A., & Kanae, S. (2015). Modeling complex flow dynamics of fluvial floods

exacerbated by sea level rise in the Ganges–Brahmaputra–Meghna Delta.

Environmental Research Letters, *10*(12), doi: 10.1088/1748-9326/10/12/124011.

James, S. L., Gubbins, P., Murray, C. J., & Gakidou, E. (2012). Developing a

comprehensive time series of GDP per capita for 210 countries from 1950 to 2015.

Population Health Metrics, *10*(1), 12, doi: 10.1186/1478-7954-10-12.

Jongman, B., Ward, P. J., & Aerts, J. C. J. H. (2012). Global exposure to river and

coastal flooding: Long term trends and changes. *Global Environmental Change*,

22(4), 823-835, doi: 10.1016/j.gloenvcha.2012.07.004.

Jonkman, S. N., Bočkarjova, M., Kok, M., & Bernardini, P. (2008). Integrated

hydrodynamic and economic modelling of flood damage in the Netherlands.

Ecological Economics, *66*(1), 77-90, doi: 10.1016/j.ecolecon.2007.12.022.

Jovel, R. J., & Mudahar, M. (2010). Damage, Loss, and Needs Assessment Guidance

Notes : Volume 3. Estimation of Post-Disaster Needs for Recovery and

Reconstruction. Report, Washington, DC.

Kinoshita, Y., Tanoue, M., Watanabe, S., & Hirabayashi, Y. (2018). Quantifying the

effect of autonomous adaptation to global river flood projections: application to

future flood risk assessments. *Environmental Research Letters*, *13*(1), doi: 10.1088/1748-9326/aa9401.

Klein G. K., & Verburg, P. H. (2013). Uncertainties in global-scale reconstructions of historical land use: an illustration using the HYDE data set. *Landscape Ecology*, *28*(5), 861-877, doi: 10.1007/s10980-013-9877-x.

Klein G. K., Beusen, A., Drecht, G. V., & Vos, M. D. (2011). The HYDE 3.1 spatially explicit database of human-induced global land-use change over the past 12,000 years. *Global Ecology and Biogeography*, *20*(1), 73-86, doi: 10.1111/j.1466-8238.2010.00587.x.

Koks, E. E., Bockarjova, M., Moel, H. d., & Aerts, J. C. (2015). Integrated Direct and Indirect Flood Risk Modeling: Development and Sensitivity Analysis. *Risk Analysis*, *35*(5), 882-900, doi: 10.1111/risa.12300.

Komori, D., Nakamura, S., Kiguchi, M., Nishijima, A., Yamazaki, D., Suzuki, S., Kawasaki, A., Oki, K., & Oki, T. (2012). Characteristics of the 2011 Chao Phraya River flood in Central Thailand. *Hydrological Research Letters*, *6*(0), 41-46, doi: 10.3178/hrl.6.41.

Kotera, A., Nagano, T., Hanittinan, P., & Koontanakulvong, S. (2015). Assessing the degree of flood damage to rice crops in the Chao Phraya delta, Thailand, using

MODIS satellite imaging. *Paddy and Water Environment*, *14*(1), 271-280, doi: 10.1007/s10333-015-0496-9.

Mateo, C. M., Hanasaki, N., Komori, D., Tanaka, K., Kiguchi, M., Champathong, A., Sukhapunnaphan, T., Yamazaki, D., & Oki, T. (2014). Assessing the impacts of reservoir operation to floodplain inundation by combining hydrological, reservoir management, and hydrodynamic models. *Water Resources Research*, *50*(9), 7245-7266, doi: 10.1002/2013wr014845.

Ministry of Land, Infrastructure, Transport and Tourism (MLIT) (2005). The flood control economy investigation manual (proposed). edited by R. Bureau, p. 91.

Ministry of Labor,http://www.mol.go.th/en/employee/interesting_information/6319

Portmann, F. T., Siebert, S., & Döll, P. (2010). MIRCA2000—Global monthly irrigated and rainfed crop areas around the year 2000: A new high‐resolution data set for agricultural and hydrological modeling. *Global Biogeochemical Cycles*, *24*(1), GB 1011, doi:10.1029/2008GB003435.

Scussolini, P., Aerts, J. C. J. H., Jongman, B., Bouwer, L. M., Winsemius, H. C., Moel, H. d., & Ward, P. J. (2016). FLOPROS: an evolving global database of flood protection standards. *Natural Hazards and Earth System Sciences*, *16*(5), 1049-1061, doi: 10.5194/nhess-16-1049-2016.

Sellers, P. J., Randall, D. A., Collatz, G. J., Berry, J. A., Field, C. B., Dazlich, D. A.,

Zhang, C., et al. (1996). A Revised Land Surface Parameterization (SiB2) for

Atmospheric GCMS. Part I: Model Formulation. *Journal of Climate*, *9*(4), 676-705,

doi: 10.1175/1520-0442(1996)009<0676:Arlspf>2.0.Co;2.

Sukegawa, S. (2012). The Sakha Ratanakon industrial park with many Japanese

companies has no levee construction - 8 months from the flood - (in Japanese).

edited, Japan External Trade Organization.

Sukegawa, S. (2013). Influences on the industries and companies and its response to the

Thailand floods in 2011 (in Japanese). Japan External Trade Organization, Chiba.

Takakura, J. y., Fujimori, S., Takahashi, K., Hasegawa, T., Honda, Y., Hanasaki, N.,

Hijioka, Y., et al. (2018). Limited Role of Working Time Shift in Offsetting the

Increasing Occupational‐Health Cost of Heat Exposure. *Earth's Future*, *6*(11),

1588-1602, doi: 10.1029/2018ef000883.

Takata, K., Emori, S., & Watanabe, T. (2003). Development of the minimal advanced

treatments of surface interaction and runoff. *Global and Planetary Change*, *38*(1-2),

209-222, doi: 10.1016/s0921-8181(03)00030-4.

Tanoue, M., Hirabayashi, Y., & Ikeuchi. H. (2016). Global-scale river flood

vulnerability in the last 50 years. *Scientific Reports*, *6*, 36021, doi:

10.1038/srep36021.

Tateishi, R., Hoan, N. T., Kobayashi, T., Alsaaideh, B., Tana, G., & Phong, D. X.

(2014). Production of Global Land Cover Data – GLCNMO2008. *Journal of*

Geography and Geology, *6*(3), doi: 10.5539/jgg.v6n3p99.

Warld Bank (2012). Thai flood 2011 : rapid assessment for resilient recovery and

reconstruction planning : Overview (English), edited, World Bank.

Willner, S. N., Otto, C., & Levermann, A. (2018). Global economic response to river

floods. *Nature Climate Change*, *8*(7), 594-598, doi: 10.1038/s41558-018-0173-2.

Winsemius, H. C., Aerts, J. C. J. H., Beek, L. P. H. v., Bierkens, M. F. P., Bouwman, A.,

Jongman, B., Kwadijk, J. C. J., et al. (2015). Global drivers of future river flood

risk. *Nature Climate Change*, *6*(4), 381-385, doi: 10.1038/nclimate2893.

Yamazaki, D., Kanae, S., Kim, H., & Oki, T. (2011). A physically based description of

floodplain inundation dynamics in a global river routing model. *Water Resources*

Research, *47*(4), doi: 10.1029/2010wr009726.